Kit-independent mast cell adhesion mediated by Notch

Akihiko Murata[1], Mari Hikosaka[2], Miya Yoshino[1], Lan Zhou[3], Shin-Ichi Hayashi[1].

[1]Division of Immunology, Department of Molecular and Cellular Biology, School of Life Science, Faculty of Medicine, Tottori University, Yonago, Tottori 683-8503, Japan

[2]Department of Stem Cell and Developmental Biology, Mie University Graduate School of Medicine, Tsu, Mie 514-8507, Japan

[3]Department of Pathology, Case Western Reserve University, Cleveland, OH 44106, USA

Corresponding author: Akihiko Murata

Division of Immunology, Department of Molecular and Cellular Biology, School of Life Science, Faculty of Medicine, Tottori University, 86 Nishi-Cho, Yonago, Tottori 683-8503, Japan

Telephone number: +81-859-38-6223

Fax number: +81-859-38-6220

E-mail address: muratako@med.tottori-u.ac.jp

Running title: Kit-independent mast cell adhesion by Notch

Keywords: Notch, Delta-like, Jagged, Mast cells, Adhesion,

The number of pages: 33

The abstract word count: 151 words

The number of figures: 7 figures and 6 supplemental figures

Abstract

Kit/CD117 plays a crucial role in the cell-cell and cell-matrix adhesion of mammalian mast cells (MCs); however, it is unclear whether other adhesion molecule(s) perform important roles in the adhesion of MCs. In the present study, we show a novel Kit-independent adhesion mechanism of mouse cultured MCs mediated by Notch family members. On stromal cells transduced with each Notch ligand gene, Kit and its signaling become dispensable for the entire adhesion process of MCs from tethering to spreading. The Notch-mediated spreading of adherent MCs involves the activation of phosphatidylinositol 3-kinases and mitogen-activated protein kinases signaling, similar to Kit-mediated spreading. Despite the activation of the same signaling pathways, while Kit supports the adhesion and survival of MCs, Notch only supports adhesion. Thus, Notch family members are specialized adhesion molecules for MCs that effectively replace the adhesion function of Kit in order to support the interaction of MCs with the surrounding cellular microenvironments.

Introduction

Mast cells (MCs) are tissue-resident immune cells that constitutively express the receptor tyrosine kinase, Kit (CD117). The differentiation and survival of MCs *in vivo* depend on Kit signaling (1-3), provided by stromal cells such as fibroblasts and endothelial cells that express the Kit ligand (Kitl) (4-7).

In addition, the crucial roles of Kit and its signaling in the cell-cell and cell-matrix adhesion of MCs have been revealed by *in vitro* adhesion assays with cultured MCs. The adhesion of floating round-shaped cultured MCs to stromal cells begins with tethering, an anchoring response that maintains the original shape. Kit and membrane-bound Kitl function as critical cell adhesion molecules mediating the tethering of cultured MCs to fibroblasts (8-11), as shown by the impaired attachment of Kit-deficient MCs to fibroblasts (8-10). The tethering of MCs by Kit-Kitl occurs in a manner that depends on their binding, but not Kit signaling, as shown by the normal attachment response of MCs harboring mutant Kit that cannot signal (8, 10).

The tethering of cultured MCs is followed by the spreading (changing the cell shape) of adherent MCs, a complex response that is considered to involve integrins and cytoskeletal reorganization (15-17). Kit signaling induces the spreading of tethered MCs through not only the activation (conformational change) of integrins that enables tethered MCs to adhere to extracellular matrices (ECMs) (15-20), but also by the induction of cytoskeletal reorganization that enables MCs to deform (21-24). These processes enable MCs to spread, and make tight contact with or migrate through the surrounding cellular and ECM environments. The Kit-induced spreading of adherent MCs involves the activation of downstream signaling pathways, including phosphatidylinositol 3-kinases (PI3K) and mitogen-activated protein kinases (MAPKs)

(17, 18, 20-24).

We previously reported that Notch family members function as cell adhesion molecules for cultured mouse MCs (25-27). Notch receptors and their canonical ligands are single-pass transmembrane signaling molecules (28-32). Humans and rodents have four Notch receptors (Notch1-Notch4) and two distinct families of canonical Notch ligands: Delta-like (Dll) ligands (Dll1, Dll3, and Dll4) and Jagged (Jag) ligands (Jag1 and Jag2). In MC biology, Notch signaling has been reported to regulate the differentiation (33-35), localization (36), and effector functions of MCs (37). When co-cultured with stromal cells transduced with each Notch ligand gene (Dll1, Dll4, Jag1, and Jag2), the adhesion of cultured MCs was markedly enhanced in a manner that depended on the interaction of each Notch ligand with Notch1 and Notch2 on MCs (25, 26). The Notch receptor-ligand interaction strongly supported the tethering of MCs to stromal cells (25, 26), but also appeared to enhance the transitioning of tethered MCs to the spreading state. However, the mechanisms by which the spreading of MCs was induced remained unclear, and whether Kit and its signaling played a role during the Notch-mediated adhesion of MCs was unknown.

In the present study, in order to reveal the requirement of Kit during the Notch-mediated adhesion of MCs, we analyzed the adhesion response of Kit-deficient MCs and the effects of an antagonistic antibody against Kit on wild-type (WT) MCs on Notch ligand-transduced stromal cells. We found that a dysfunction in Kit in MCs had negligible suppressive effects on the entire adhesion process of MCs from tethering to spreading on Notch ligand-transduced stromal cells. The Kit-independent spreading of adherent MCs on Notch ligand-transduced stromal cells involved the activation of the MAPKs and PI3K pathways, similar to the Kit-dependent adhesion of WT MCs on

normal stromal cells. Our results showed the presence of a Kit-independent adhesion mechanism of MCs mediated by Notch family members.

Methods

Mice

C57BL/6J mice were purchased from Japan CLEA (Tokyo, Japan). C57BL/6J-*Kit*$^{+/W\text{-}sh}$ mice (RBRC01888) were provided by RIKEN BRC (Ibaraki, Japan) through the National Bio-Resource Project of MEXT, Japan, and were bred to obtain C57BL/6J-*Kit*$^{+/+}$ and -*Kit*$^{W\text{-}sh/W\text{-}sh}$ mice. Mice were maintained in a specific pathogen-free facility in Tottori University. Experiments were approved by and performed in accordance with the guidelines of the Animal Care and Use Committee of Tottori University.

Bone marrow-derived cultured MCs

Cells from femora were cultured in minimum essential medium alpha (MEMα; Gibco-BRL, Grand Island, NY) supplemented with 10% fetal bovine serum (FBS, JRH Biosciences, Lenexa, KS), antibiotics (penicillin and streptomycin, Meiji Seika, Tokyo, Japan), and 50 U/mL culture supernatant of Chinese hamster ovary cells producing recombinant mouse interleukin (IL)-3 (a gift from Dr. Sudo, Toray Industries, Inc., Kanagawa, Japan) in a humidified atmosphere with 5% CO_2 at 37°C. Non-adherent cells were placed into fresh media every 5-7 days. After more than 8 weeks, more than 97% of cells were MCs, as judged by the surface expression of Kit and FcεRIα with flow cytometry (25, 26). In Figure 1A, MCs obtained from C57BL/6J mice (Japan CLEA) were used. In other experiments, MCs from age- and sex-matched pairs of

C57BL/6J-*Kit*$^{+/+}$ and -*Kit*$^{W\text{-}sh/W\text{-}sh}$ mice (RIKEN BRC) were used.

Stromal Cells

OP9 stromal cell lines transduced with the mouse Dll1, Dll3, Dll4, Jag1, or Jag2 gene (OP9-Dll1, -Dll3, -Dll4, -Jag1 or -Jag2) and control OP9-Ret10 cells (OP9-Ctrl) were as described previously (38). All OP9 cells expressed the green fluorescent protein (GFP). They were cultured with MEMα supplemented with 20% FBS and antibiotics.

Antibodies

The following monoclonal antibodies (mAbs) were used in flow cytometry: FITC-conjugated anti-mouse Kit (ACK2, Tonbo Biosciences, San Diego, CA) (39), PE-conjugated anti-mouse FcεRIα (MAR-1), and CD49b (DX5) (eBioscience, San Diego, CA).

Unlabeled ACK2, anti-mouse IL-7Rα (A7R34), and anti-mouse Gr-1 (RB6-8C5) mAb dissolved in PBS were used in cell cultures (all made in-house). Purified sheep anti-mouse Notch1 (AF5267) or Notch2 (AF5196) polyclonal Abs (pAbs) and sheep control IgG (5-001-A) were purchased from R&D Systems (Minneapolis, MN).

Reagents

Sodium azide (NaN_3), dimethylsulfoxide (DMSO), SB203580, SP600125, and

PD98059 (Wako Pure Chemical Industries, Osaka, Japan), LY294002 (Merck Millipore, Darmstadt, Germany), *N*-[*N*-(3,5-difluorophenacetyl)-L-alanyl]-S-phenylglycine t-butyl ester (DAPT) (Peptide Institute, Osaka, Japan), and cytochalasin D (Sigma-Aldrich, St Louis, MO) were used.

Reverse transcriptase-polymerase chain reaction (RT-PCR)

A RT-PCR analysis was performed as previously described (26). Briefly, synthesized cDNA (equivalent to 25 ng total RNA) was amplified using rTaq DNA polymerase and TaKaRa PCR Thermal Cycler Dice® Gradient (Takara, Shiga, Japan). Primers were as described: *Kit* (40), *Fcer1a* (41), and *Kitl* (25).

Adhesion assay

OP9 stromal cells (1.6×10^4 for 48-well plates (for Figure 1A) and 5.0×10^3 for 96-well plates (for other experiments)) were seeded in the wells of 48- or 96-well flat-bottomed culture plates (Corning) and cultured for 2 days in order to prepare confluent monolayers. After washing OP9 cells once with phosphate-buffered saline (PBS), MCs suspended in MEMα with 10% FBS were seeded onto the wells (1.5×10^5 in 100 μL for 48-well plates and 5.0×10^4 in 50 μL for 96-well plates) with or without reagents, and incubated at 37ºC for 60 min. In adhesion assays with inhibitors (SB203580, SP600125, PD98059 LY294002, and DAPT), MCs were pre-treated with the inhibitors at room temperature for 10 - 60 min, and then seeded onto OP9 cells with inhibitors. The culture supernatant was recovered after agitation (low speed, scale 5) for 30 sec with a

MicroMixer E-36 (Taitec corporation, Saitama, Japan), and non-adherent MCs in the supernatants were counted with hemocytometers. The percentages and numbers of adherent MCs relative to those initially added were calculated.

In the assay with fixed stromal cells, confluent monolayers of each OP9 cell were fixed with 2% paraformaldehyde (PFA, Wako) at room temperature for 5 min. After washing wells three times with PBS, the adhesion assay was performed.

In the evaluation of the adhesion states of MCs, photomicrographs (magnification: ×200) of each well (avoiding the center of the wells at which adherent MCs were very dense) were taken immediately after the removal of the supernatant. The numbers of adherent MCs in each adhesion state in a chosen area (1000×1000~1200×1200 pixels) in a well were counted, and the numbers of adherent MCs in each state were calculated.

Survival assay

OP9 stromal cells (3×10^4 for 24-well plates (for Figure 6B and 6C) and 1.5×10^4 for 48-well plates (for other experiments)) were seeded on the 0.1% type A gelatin (Sigma-Aldrich)-coated wells of 24-well or 48-well flat-bottomed culture plates (Corning). The next day, MCs (1.5×10^5 in 500 μL for 24-well plates and 7.5×10^4 in 200 μL for 48-well plates) suspended in MEMα with 10% FBS were seeded on the sub-confluent OP9 monolayer with or without reagents, and were cultured at 37°C for 7 days. On day 4, 1× volume of fresh media without or with inhibitors (1× concentration) were added. On day 7, all cells in a well were recovered by trypsinization, stained with propidium iodide (PI, Sigma-Aldrich) to exclude dead cells, and suspended in the same

volume of buffer. Cells were analyzed with the flow cytometer EPICS XL (Coulter, Palo Alto, CA) under the same flow rate for 60 sec. GFP-positive cells (OP9 cells) were excluded and live MCs (PI^-GFP^-) were counted using WinMDI ver 2.9 software (Purdue University, West Lafayette, IN). The percentages of live MCs relative to those initially added, which were analyzed with the same methods on day 0, were calculated.

Flow cytometry

Hank's solution (Nissui Pharmaceutical, Tokyo, Japan) containing 2.5% heat-inactivated FBS and 0.02% NaN_3 was used as staining buffer. Cells were initially incubated with 33% rabbit serum (Gibco) with anti-CD16/32 (2.4G2, Tonbo Biosciences) for blocking, and then stained with fluorescein-labeled mAbs and PI. Regarding the detection of Notch receptors in Figure 1D, cells were stained with fluorescein-labeled mAbs and sheep control, anti-mouse Notch1, or anti-mouse Notch2 pAbs (R&D Systems), and then with rabbit anti-sheep IgG-biotin (Vector Laboratories) and streptavidin-PE (SouthernBiotech). Cells were analyzed with EPICS XL and WinMDI software.

Statistical analysis

Each experiment was repeated more than twice, with similar results being obtained each time, and representative results were shown unless otherwise indicated. Statistical analyses were performed in Microsoft Excel (for Welch's *t*-test) and IBM SPSS Statistics version 25 (for a one-way ANOVA with post-hoc tests). The significance of differences was established at $p < 0.05$.

Results

Kit was dispensable for the adhesion of MCs to Notch ligand-transduced stromal cells

In order to examine the role of Kit during Notch-mediated MC adhesion, WT cultured MCs were incubated on a confluent monolayer of OP9 stromal cells transduced with each Notch ligand gene (OP9-Dll1, -Dll4, -Jag1, and -Jag2) (26, 38), with or without ACK2, an antagonistic mAb against mouse Kit. In the presence of a control mAb, the adhesion of MCs was more strongly promoted on OP9-Dll1, -Dll4, -Jag1, or -Jag2 than the responses on OP9-Ctrl (Figure 1A, open circles). The addition of ACK2 significantly inhibited the adhesion of MCs to OP9-Ctrl cells, but had a negligible effect on adhesion to OP9 cells transduced with Notch ligands (Figure 1A).

We then assessed cultured MCs obtained from C57BL/6-$Kit^{+/+}$ and -$Kit^{W\text{-}sh/W\text{-}sh}$ mice (hereafter MCs-$Kit^{+/+}$ and -$Kit^{W\text{-}sh/W\text{-}sh}$) (Supplemental Figure 1). W^{sh} is an inversion mutation in the transcriptional regulatory elements upstream of the *Kit* transcription start site (37). Therefore, MCs-$Kit^{W\text{-}sh/W\text{-}sh}$ failed to express the *Kit* (9), but not *Fcer1a* transcript (Figure 1B and supplemental Figure 1). The adhesion of MCs-$Kit^{W\text{-}sh/W\text{-}sh}$ to OP9-Ctrl cells at 60 min of the adhesion assay was significantly weaker than that of MCs-$Kit^{+/+}$ (Figure 1C). In contrast, the promoted adhesion of MCs to OP9-Dll1, -Dll4, -Jag1, and -Jag2 was not influenced by the insufficiency of Kit expression (Figure 1C). MCs-$Kit^{+/+}$ and -$Kit^{W\text{-}sh/W\text{-}sh}$ were both immature (Supplemental Figure 2) and expressed Notch1 and Notch2 on their surfaces (Figure 1D). Mature peritoneal MCs from C57BL/6 mice also expressed Notch1 and Notch2 (Figure 1D and Supplemental Figure 2), suggesting that the expression of Notch receptors is maintained

throughout the maturation of MCs. MCs-*Kit*$^{W\text{-}sh/W\text{-}sh}$ did not express *Kit* mRNA after a 60-min co-culture with each OP9 transductant (Figure 1E) and every OP9 transductant expressed *Kitl*, but not *Kit* or *Fcer1a* mRNA (Figure 1F and Supplemental Figure 3).

These results showed that the lack of the Kit-Kitl interaction did not affect the adhesion of MCs to Notch ligand-transduced stromal cells.

Spreading of adherent MCs on Notch ligand-transduced stromal cells was affected less by the insufficiency of Kit in MCs

Kit signaling induces cytoskeletal reorganization, leading to changes in the cell morphology of adherent MCs (21-23). In our adhesion assay, while some adherent MCs maintained their original morphology (spherical and refractile), some adherent MCs spread on stromal cells with deformed shapes and appeared dark under phase-contrast microscopy (Figure 2A). In cultures with the inhibition of cellular metabolism by NaN_3 (a mitochondrial F-ATPase inhibitor) (43) or on ice, and in the presence of cytochalasin D (an actin polymerization inhibitor), deformed MCs were not observed and most of the adherent MCs maintained their original morphology (Figure 2B). Therefore, deformed and dark-looking adherent MCs represented an advanced stage of cell adhesion accompanied by cytoskeletal reorganization.

Using photomicrographs of adherent MCs after the removal of floating cells, we assessed the numbers of adherent MCs in each adhesion state, i.e., refractile ones as in tethering, dark ones as in spreading, and intermediate ones as in a transitional stage (Figure 2A). In the adhesion assay for MCs-*Kit*$^{+/+}$ on OP9-Ctrl cells, the ratio and number of spreading MCs were gradually increased and maximized at 60-120 min

(Figure 2C and 2D). In contrast, MCs-*Kit*$^{W\text{-}sh/W\text{-}sh}$ showed an impaired transition from the tethering to spreading state (Figure 2C and 2D), demonstrating the importance of Kit signaling in this process. The kinetics of the adhesion states of MCs-*Kit*$^{+/+}$ on OP9-Dll1, -Dll4, -Jag1, and -Jag2 were similar to that on OP9-Ctrl, except that the numbers of transitioning plus spreading MCs were higher (Figure 2E).

We compared the numbers of adherent MCs in each state at 60 min between MCs-*Kit*$^{+/+}$ and MCs-*Kit*$^{W\text{-}sh/W\text{-}sh}$ (Figure 3A and 3B). MCs-*Kit*$^{+/+}$ showed higher cell numbers in the transitioning plus spreading states on OP9-Dll1, -Dll4, and -Jag1 than those on OP9-Ctrl (Figure 3B, each left bars). The numbers of spreading MCs-*Kit*$^{+/+}$ on OP9-Dll4 and -Jag1 were significantly higher than that on OP9-Ctrl cells in some (but not all) experiments. In contrast to the response on OP9-Ctrl cells, the lack of Kit in MCs-*Kit*$^{W\text{-}sh/W\text{-}sh}$ only had a small inhibitory or no effect on their transition from the tethering to spreading states on Notch ligand-transduced OP9 cells (Figure 3B). Moreover, the treatment with ACK2 during the adhesion assay did not markedly affect the spreading response of MCs-*Kit*$^{+/+}$ on Notch ligand-transduced OP9 cells (Figure 3C).

These results indicate that the spreading of adherent MCs on OP9-Ctrl cells required Kit signaling, whereas that on Notch ligand-transduced stromal cells mostly occurred in a Kit-independent manner.

Spreading of MCs-Kit$^{W\text{-}sh/W\text{-}sh}$ *on Notch ligand-transduced stromal cells occurred in a manner depending on the Notch receptor-ligand interaction, but not canonical Notch signaling*

We hypothesized that Notch receptors on MCs functioned not only as cell adhesion molecules mediating the tethering of MCs (25, 26), but also induced the subsequent spreading of adherent MCs via Notch signaling. In canonical signaling, Notch receptor-ligand binding between neighboring cells ultimately induces the proteolytic cleavage of the receptor by the γ-secretase complex. This permits the Notch intracellular domain to translocate into the nucleus, in which it induces the transcription of Notch target genes (28-32). MCs mainly express Notch2 and, to a lesser extent, Notch1, both of which cooperatively function in the Notch-mediated adhesion of MCs (26). The treatment with anti-Notch1 plus anti-Notch2 pAbs during the adhesion assay for MCs-$Kit^{W\text{-}sh/W\text{-}sh}$ significantly reduced the numbers of adherent MCs in each adhesion state on each Notch ligand-transduced OP9 cell (Figure 4A). The treatment of these pAbs did not affect the adhesion states of MCs-$Kit^{W\text{-}sh/W\text{-}sh}$ on OP9-Ctrl cells. Thus, the initiation of the entire adhesion process of MCs-$Kit^{W\text{-}sh/W\text{-}sh}$ depended on the Notch receptor-ligand interactions on Notch ligand-transduced OP9 cells.

We then tested whether the treatment with the canonical Notch signaling inhibitor, DAPT (γ-secretase inhibitor) inhibited the spreading of adherent MCs. The treatment with 50 μM DAPT had no effect on the adhesion states of MCs-$Kit^{W\text{-}sh/W\text{-}sh}$ on each OP9 cell (Figure 4B). The spreading of MCs-$Kit^{+/+}$ on each OP9 cell in the presence of ACK2 was also not suppressed by the additional treatment with DAPT (Figure 4C). We previously confirmed that the treatment of 10 μM DAPT was sufficient to reverse the activation of transcription of Notch target genes (*Hes1* and *Hey1*) in WT MCs cultured on OP9-Dll1 (26).

These results indicated that the spreading of adherent MCs-$Kit^{W\text{-}sh/W\text{-}sh}$ in Notch-mediated cell adhesion was dependent on the Notch receptor-ligand interaction,

but independent of canonical Notch signaling mediated by γ-secretase activity.

Kit-independent spreading of adherent MCs-Kit$^{W\text{-}sh/W\text{-}sh}$ on Notch ligand-transduced stromal cells involved the activation of MAPKs and PI3K pathways

Kit signaling activates PI3K and three MAPKs pathways: p38 MAPKs, extracellular signal-regulated kinases (ERKs), and c-Jun amino-terminal kinases (JNKs) (44-47). These signaling pathways mediate the Kit-induced cytoskeletal reorganization of adherent MCs (21-23). Consistent with these findings, the numbers of the Kit-dependent spreading of adherent MCs-*Kit*$^{+/+}$ on OP9-Ctrl cells were significantly reduced, and tethering was increased by the treatment with inhibitors for p38 (SB203580), JNKs (SP600125), ERK1/2 (PD98059), and PI3K (LY294002) (Figure 5A).

Treatments with these inhibitors also significantly impaired the spreading, and increased the tethering of MCs-*Kit*$^{W\text{-}sh/W\text{-}sh}$ on OP9-Dll4 cells (Figure 5B and 5D) and other Notch ligand-transduced OP9 cells (Supplemental Figure 4). In order to exclude the effects of these inhibitors on stromal cells, we performed the adhesion assay on 2% PFA-fixed OP9-Dll4 cells. The spreading of adherent MCs-*Kit*$^{W\text{-}sh/W\text{-}sh}$ was also significantly inhibited and most of the adherent MCs were tethering by the treatment with these inhibitors (Figure 5C and 5D).

These results suggested that on Notch ligand-transduced stromal cells, MAPKs (p38, JNK and ERK) and PI3K pathways were all activated, even in Kit-deficient MCs, directing the effective spreading of adherent MCs.

Notch receptor-ligand interactions did not support the survival of MCs-Kit$^{W\text{-}sh/W\text{-}sh}$

On fibroblasts expressing Kitl, while WT MCs survive over the long term, MCs lacking functional Kit cannot survive and disappear from the culture (8, 9). Kit signaling prevents the apoptosis of cultured MCs in a manner depending on the activation of the PI3K and ERKs pathways (48, 49). Since the PI3K and MAPKs pathways in MCs were activated in a Kit-independent manner on Notch ligand-transduced OP9 cells, we investigated whether Notch ligand-transduced OP9 cells support the survival of Kit-deficient MCs.

After culturing MCs-$Kit^{+/+}$ or -$Kit^{W\text{-}sh/W\text{-}sh}$ on each OP9 transductant for 7 days, the number of live MCs-$Kit^{W\text{-}sh/W\text{-}sh}$ was significantly lower than that of MCs-$Kit^{+/+}$ on every OP9 transductant (Figure 6A and Supplemental Figure 5A). Any improvement in the survival of MCs-$Kit^{W\text{-}sh/W\text{-}sh}$ on every Notch ligand-transduced OP9 cell was not observed from their response on OP9-Ctrl (Figure 6A). Without OP9 stromal cells, neither MCs-$Kit^{+/+}$ nor -$Kit^{W\text{-}sh/W\text{-}sh}$ survived (Figure 6A, OP9(-)). The survival responses of MCs-$Kit^{+/+}$ on OP9-Dll4 and -Jag2 were slightly weaker than those on OP9-Ctrl (Figure 6A), and were improved in the presence of DAPT in 3 out of 3 or 1 out of 3 experiments, respectively (Supplemental Figure 5B), suggesting that Notch signaling exerts negative effects on the survival of MCs. Histocytochemistry showed that granule contents in MCs-$Kit^{+/+}$ cultured on every OP9 transductant remained in the immature state (Supplemental Figure 6). The survival of MCs-$Kit^{+/+}$ on OP9-Ctrl depended on Kit signaling because the treatment with ACK2 reduced their survival to the level of MCs-$Kit^{W\text{-}sh/W\text{-}sh}$ (Figure 6B). In addition, the survival of MCs-$Kit^{+/+}$ on OP9-Ctrl was impaired by the inhibition of PI3K (LY294002) and, to a lesser extent, p38 (SB203580) and ERK1/2 (PD98059) (Figure 6C), showing the involvement of these signaling

pathways in the Kit-dependent survival of MCs. The effects of the JNK inhibitor (SP600125) were unclear because of its toxicity against stromal cells in this long-term culture (data not shown).

These results suggested that although Notch ligand-transduced stromal cells effectively supported the entire adhesion process of Kit-deficient MCs from tethering to spreading, with the latter process involving the activation of the PI3K and MAPKs pathway, they were unable to support the survival of MCs-$Kit^{W\text{-}sh/W\text{-}sh}$. Thus, Notch family members were specialized molecules for the mediation of the cell adhesion of MCs, while Kit supported the survival and adhesion of MCs (Figure 7).

Discussion

We herein demonstrated the existence of a Kit-independent adhesion mechanism for mammalian MCs mediated by Notch family members (Figure 7). On Notch ligand-transduced stromal cells, not only was the entire adhesion process of cultured MCs from tethering to spreading effectively induced in a manner depending on the Notch receptor-ligand interaction, but Kit became dispensable to this process. Thus, the Notch-mediated adhesion of MCs is a novel mode of MC interaction with the surrounding microenvironments.

A small number of Kit-deficient MCs still adhered to OP9-Ctrl cells. Although OP9-Ctrl cells weakly expressed endogenous Jag1 on their surface (26), it did not contribute to the adhesion of MCs (ref. 26 and Figure 4A), suggesting that other adhesion molecules, such as ICAM1 and VCAM1, expressed by OP9 cells (25) are involved in this process. This result also indicates that Notch ligands require a certain level of surface expression to induce MC adhesion. Our results suggested that when expression exceeds a certain level, the functions of the Notch-mediated and Kit-mediated adhesion pathways become redundant.

The Notch-mediated spreading of adherent MCs involved the activation of PI3K and MAPKs (p38, JNK, ERK), similar to Kit-mediated spreading. However, it is unclear how these pathways are activated in Kit-deficient MCs during Notch-mediated adhesion. Since γ-secretase activity, which is essential for canonical Notch signaling, was dispensable for the induction of spreading, the γ-secretase-independent non-canonical Notch signaling pathway may be involved (50-52). Previous studies suggested the direct activation of the PI3K pathway by non-canonical Notch signaling

(53-55). In contrast, although Notch signaling has been shown to indirectly regulate MAPKs signaling activated by other cell surface receptors (56-66), there does not appear to be any evidence of direct MAPKs activation by non-canonical Notch signaling. Therefore, one possible mechanism for Notch-mediated spreading is that non-canonical Notch signaling directly activates PI3K and indirectly enhances MAPKs pathways in tethered MCs, leading to cytoskeletal reorganization for deforming (Figure 7).

Notch ligand-rich environments did not support the survival of Kit-deficient MCs despite their capacities to activate the MAPKs and PI3K pathways in adherent MCs. Kit-mediated MC survival involves the down-regulation of pro-apoptotic BCL-2 family members (Bim and Puma) by a series of reactions starting from activated PI3K and ERK (48, 49). Thus, the Notch-mediated activation of these signaling pathways may not lead to the down-regulation of Bim or Puma. Although it currently remains unclear why this qualitative difference between the Kit- and Notch-mediated activation of PI3K and ERK occurs, Notch family members appear to be specialized molecules that induce cell adhesion, while Kit supports the adhesion and survival of MCs.

The physiological conditions under which Notch-mediated MC adhesion is operating remain unknown; however, this adhesion will enable MCs to maintain or to form cell-cell and cell-ECM adhesion with cells not expressing Kitl, but expressing Notch ligands, or when Kit-mediated adhesion becomes dysfunctional. There are some inhibitory mechanisms of Kit-mediated MC responses. The binding of Kitl induces the internalization of surface Kit on MCs (67, 68) and the activation of MCs induces the shedding of the Kit ectodomain through the activation of proteases (67-69), both of which result in the impaired adhesion of MCs to fibroblasts (68). Moreover, blood

plasma contains a higher level of the soluble Kit ectodomain than soluble Kitl (70), and soluble Kit inhibits Kitl bioactivity by acting as a decoy (71). One possible condition under which Notch-mediated adhesion functions is chronic inflammation, in which Notch ligands are up-regulated in stromal cells (72-76) and MCs frequently accumulate (77). Therefore, the activation of tissue MCs and increased vascular permeability may lead to impaired Kit-mediated MC adhesion. Notch-mediated adhesion may provide an advantage to MCs harboring reduced surface Kit for their interactions with and migration through the surrounding cellular environments.

In mice, the niche retention of hematopoietic stem cells (HSCs) in bone marrow was recently suggested to involve Notch-mediated cell adhesion (78, 79). Since HSCs express Kit and Notch receptors as MCs, further studies are warranted in order to examine the relationship between these two receptors in niche retention based on our results. Moreover, since the expression of Notch receptors is considered to be maintained throughout the differentiation of diverse immune cell lineages (28, 30), the role of Notch-mediated cell adhesion in various Notch-dependent responses throughout life needs to be examined.

Funding

This work was supported by JSPS KAKENHI Grant Numbers 25860295, 15K19076, and 18K08297 (to A.M.) and 26460488 (to S.I.H.), and Takeda Science Foundation (to A.M.).

Acknowledgments

We thank Dr. Yukihiko Kitamura for his kind reading of and provision of comments on the manuscript, Dr. Tetsuo Sudo (Toray Industries) and Dr. Keigo Nishida (Suzuka University of Medical Science, Mie, Japan) for materials, and Ms. Toshie Shinohara for her technical assistance.

Conflicts of Interest

We declare no conflicts of interest.

References

1. Kitamura, Y., Oboki, K. and Ito, A. 2007. Development of mast cells. *Proc. Jpn. Acad. Ser. B Phys. Biol. Sci.* 83:164.

2. Galli, S.J., Tsai, M., Marichal, T., Tchougounova, E., Reber, L.L. and Pejler, G. 2015. Approaches for analyzing the roles of mast cells and their proteases in vivo. *Adv. Immunol.* 126:45.

3. Galli, S.J. 2016. The Mast Cell-IgE Paradox: From Homeostasis to Anaphylaxis. *Am. J. Pathol.* 186:212.

4. Flanagan, J.G., Chan, D.C. and Leder, P. 1991. Transmembrane form of the kit ligand growth factor is determined by alternative splicing and is missing in the Sld mutant. *Cell* 64:1025.

5. Huang, E., Nocka, K., Beier, D.R. *et al.* 1990. The hematopoietic growth factor KL is encoded by the Sl locus and is the ligand of the c-kit receptor, the gene product of the W locus. *Cell* 63:225.

6. Zsebo, K.M., Williams, D.A., Geissler, E.N. *et al.* 1990. Stem cell factor is encoded at the Sl locus of the mouse and is the ligand for the c-kit tyrosine kinase receptor. *Cell* 63:213.

7. Miyamoto, T., Sasaguri, Y., Sasaguri, T. *et al.* 1997. Expression of stem cell factor in human aortic endothelial and smooth muscle cells. *Atherosclerosis* 129:207.

8. Adachi, S., Ebi, Y., Nishikawa, S. *et al.* 1992. Necessity of extracellular domain of W (c-kit) receptors for attachment of murine cultured mast cells to fibroblasts. *Blood* 79:650.

9. Tono, T., Tsujimura, T., Koshimizu, U. *et al.* 1992. c-kit gene was not transcribed in cultured mast cells of mast cell-deficient Wsh/Wsh mice that have a normal number of erythrocytes and a normal c-kit coding region. *Blood* 80:1448.

10. Koma, Y., Ito, A., Watabe, K. *et al.* 2005. Distinct role for c-kit receptor tyrosine

kinase and SgIGSF adhesion molecule in attachment of mast cells to fibroblasts. *Lab. Invest.* 85:426.

11. Tabone-Eglinger, S., Calderin-Sollet, Z., Pinon, P. *et al.* 2014. Niche anchorage and signaling through membrane-bound Kit-ligand/c-kit receptor are kinase independent and imatinib insensitive. *FASEB J.* 28:4441.

12. Huveneers, S and Danen, E.H. 2009. Adhesion signaling - crosstalk between integrins, Src and Rho. *J. Cell Sci.* 122:1059.

13. Shen, B., Delaney, M.K. and Du, X. 2012. Inside-out, outside-in, and inside-outside-in: G protein signaling in integrin-mediated cell adhesion, spreading, and retraction. *Curr. Opin. Cell Biol.* 24:600.

14. Wolfenson, H., Iskratsch, T. and Sheetz, M.P. 2014. Early events in cell spreading as a model for quantitative analysis of biomechanical events. *Biophys J.* 107:2508.

15. Kinashi, T. and Springer, T.A. 1994. Steel factor and c-kit regulate cell-matrix adhesion. *Blood* 83:1033.

16. Dastych, J. and Metcalfe, D.D. 1994. Stem cell factor induces mast cell adhesion to fibronectin. *J. Immunol.* 152:213.

17. Serve, H., Yee, N.S., Stella, G., Sepp-Lorenzino, L., Tan, J.C. and Besmer, P. 1995. Differential roles of PI3-kinase and Kit tyrosine 821 in Kit receptor-mediated proliferation, survival and cell adhesion in mast cells. *EMBO J.* 14:473.

18. Vosseller, K., Stella, G., Yee, N.S. and Besmer, P. 1997. c-kit receptor signaling through its phosphatidylinositide-3'-kinase-binding site and protein kinase C: role in mast cell enhancement of degranulation, adhesion, and membrane ruffling. *Mol. Biol. Cell* 8:909.

19. Tan, B.L., Yazicioglu, M.N., Ingram, D. *et al.* 2003. Genetic evidence for convergence of c-Kit- and alpha4 integrin-mediated signals on class IA PI-3kinase and the Rac pathway in regulating integrin-directed migration in mast cells. *Blood* 101:4725.

20. Ali, K., Bilancio, A., Thomas, M. *et al.* 2004. Essential role for the p110delta phosphoinositide 3-kinase in the allergic response. *Nature* 431:1007.

21. Sivalenka, R.R. and Jessberger, R. 2004. SWAP-70 regulates c-kit-induced mast cell activation, cell-cell adhesion, and migration. *Mol. Cell Biol.* 24:10277.

22. Samayawardhena, L.A., Kapur, R. and Craig, A.W. 2007. Involvement of Fyn kinase in Kit and integrin-mediated Rac activation, cytoskeletal reorganization, and chemotaxis of mast cells. *Blood* 109:3679.

23. Mani, M., Venkatasubrahmanyam, S., Sanyal, M. *et al.* 2009. Wiskott-Aldrich syndrome protein is an effector of Kit signaling. *Blood* 114:2900.

24. Dráber, P., Sulimenko, V. and Dráberová, E. 2012. Cytoskeleton in mast cell signaling. *Front. Immunol.* 3:130.

25. Murata, A., Okuyama, K., Sakano, S. *et al.* 2010. A Notch ligand, Delta-like 1 functions as an adhesion molecule for mast cells. *J. Immunol.* 185:3905.

26. Murata, A., Yoshino, M., Hikosaka, M. *et al.* 2014. An evolutionary-conserved function of mammalian notch family members as cell adhesion molecules. *PLoS One* 9:e108535.

27. Murata, A. and Hayashi, S.I. 2016. Notch-mediated cell adhesion. *Biology(Basel)* 5: 5.

28. Yuan, J.S., Kousis, P.C., Suliman, S., Visan, I. and Guidos, C.J. 2010. Functions of notch signaling in the immune system: consensus and controversies. *Annu. Rev. Immunol.* 28:343.

29. Guruharsha, K.G., Kankel, M.W. and Artavanis-Tsakonas, S. 2012. The Notch signalling system: recent insights into the complexity of a conserved pathway. *Nat. Rev. Genet.* 13:654.

30. Radtke, F., MacDonald, H.R., Tacchini-Cottier, F. 2013. Regulation of innate and

adaptive immunity by Notch. *Nat. Rev. Immunol.* 13:427.

31. LaFoya, B., Munroe, J.A., Mia, M.M. *et al.* 2016. Notch: A multi-functional integrating system of microenvironmental signals. *Dev. Biol.* 418:227.

32. Kovall, R.A., Gebelein, B., Sprinzak, D. and Kopan, R. 2017. The Canonical Notch Signaling Pathway: Structural and Biochemical Insights into Shape, Sugar, and Force. *Dev. Cell* 41:228.

33. Sakata-Yanagimoto, M., Nakagami-Yamaguchi, E., Saito, T. *et al.* 2008. Coordinated regulation of transcription factors through Notch2 is an important mediator of mast cell fate. *Proc. Natl. Acad. Sci. USA* 105:7839.

34. Da'as, S.I., Coombs, A.J., Balci, T.B., Grondin, C.A., Ferrando, A.A. and Berman, J.N. 2012. The zebrafish reveals dependence of the mast cell lineage on Notch signaling in vivo. *Blood* 119:3585.

35. Honjo, A., Nakano, N., Yamazaki S. *et al.* 2017. Pharmacologic inhibition of Notch signaling suppresses food antigen-induced mucosal mast cell hyperplasia. *J. Allergy Clin. Immunol.* 139:987.

36. Sakata-Yanagimoto, M., Sakai, T., Miyake, Y. *et al.* 2011. Notch2 signaling is required for proper mast cell distribution and mucosal immunity in the intestine. *Blood* 117:128.

37. Nakano, N., Nishiyama, C., Yagita, H. *et al.* 2015. Notch signaling enhances FcεRI-mediated cytokine production by mast cells through direct and indirect mechanisms. *J. Immunol.* 194:4535.

38. Zhou, L., Li, L.W., Yan, Q. *et al.* 2008. Notch-dependent control of myelopoiesis is regulated by fucosylation. *Blood* 112:308.

39. Ogawa, M., Matsuzaki, Y., Nishikawa S. *et al.* 1991. Expression and function of *c-kit* in hemopoietic progenitor cells. *J. Exp. Med.* 174:63.

40. Hayashi, S.I., Kunisada, T., Ogawa, M., Yamaguchi, K. and Nishikawa, S.I. 1991.

Exon skipping by mutation of an authentic splice site of c-kit gene in W/W mouse. *Nucleic Acids Res.* 19:1267.

41. Hikosaka, M., Murata, A., Yoshino, M. and Hayashi S.I. 2017. Correlation between cell aggregation and antibody production in IgE-producing plasma cells. *Biochemistry and Biophysics Reports* 10:224.

42. Nagle, D.L., Kozak, C.A., Mano, H., Chapman, V.M. and Bućan, M. 1995. Physical mapping of the Tec and Gabrb1 loci reveals that the W^{sh} mutation on mouse chromosome 5 is associated with an inversion. *Hum. Mol. Genet.* 4:2073.

43. Bowler, M.W., Montgomery, M.G., Leslie, A.G. and Walker, J.E. 2006. How azide inhibits ATP hydrolysis by the F-ATPases. *Proc. Natl. Acad. Sci. USA* 103:8646.

44. Ishizuka, T., Chayama, K., Takeda, K. *et al.* 1999. Mitogen-activated protein kinase activation through Fc epsilon receptor I and stem cell factor receptor is differentially regulated by phosphatidylinositol 3-kinase and calcineurin in mouse bone marrow-derived mast cells. *J. Immunol.* 162:2087.

45. Reber, L., Da Silva, C.A. and Frossard, N. 2006. Stem cell factor and its receptor c-Kit as targets for inflammatory diseases. *Eur. J. Pharmacol.* 533:327.

46. McDaniel, A.S., Allen, J.D., Park, S.J. *et al.* 2008. Pak1 regulates multiple c-Kit mediated Ras-MAPK gain-in-function phenotypes in Nf1+/- mast cells. *Blood* 112:4646.

47. Lennartsson, J. and Rönnstrand, L. 2012. Stem cell factor receptor/c-Kit: from basic science to clinical implications. *Physiol. Rev.* 92:1619.

48. Möller, C., Alfredsson, J., Engström, M. *et al.* 2005. Stem cell factor promotes mast cell survival via inactivation of FOXO3a-mediated transcriptional induction and MEK-regulated phosphorylation of the proapoptotic protein Bim. *Blood* 106:1330.

49. Ekoff, M., Kaufmann, T., Engström, M. *et al.* 2007. The BH3-only protein Puma plays an essential role in cytokine deprivation induced apoptosis of mast cells. *Blood* 110:3209.

50. Andersen, P., Uosaki, H., Shenje, L.T. and Kwon, C. 2012. Non-canonical Notch signaling: emerging role and mechanism. *Trends Cell Biol.* 22:257.

51. Minter, L.M. and Osborne, B.A. 2012. Canonical and non-canonical Notch signaling in $CD4^+$ T cells. *Curr. Top. Microbiol. Immunol.* 360:99.

52. Ayaz, F. and Osborne, B.A. 2014. Non-canonical notch signaling in cancer and immunity. *Front. Oncol.* 4:345.

53. Gentle, M.E., Rose, A., Bugeon, L. and Dallman, M.J. 2012. Noncanonical Notch signaling modulates cytokine responses of dendritic cells to inflammatory stimuli. *J. Immunol.*189:1274.

54. Perumalsamy, L.R., Nagala, M., Banerjee, P. and Sarin, A. 2009. A hierarchical cascade activated by non-canonical Notch signaling and the mTOR-Rictor complex regulates neglect-induced death in mammalian cells. *Cell Death Differ.* 16:879.

55. Sade, H., Krishna, S. and Sarin, A. 2004. The anti-apoptotic effect of Notch-1 requires p56lck-dependent, Akt/PKB-mediated signaling in T cells. *J. Biol. Chem.* 279:2937.

56. Wang, W., Prince, C.Z., Mou, Y. and Pollman, M.J. 2002. Notch3 signaling in vascular smooth muscle cells induces c-FLIP expression via ERK/MAPK activation. Resistance to Fas ligand-induced apoptosis. *J. Biol. Chem.* 277:21723.

57. Sundaram, M.V. 2005. The love-hate relationship between Ras and Notch. *Genes Dev.* 19:1825.

58. Doroquez, D.B. and Rebay, I. 2006. Signal integration during development: mechanisms of EGFR and Notch pathway function and cross-talk. *Crit. Rev. Biochem. Mol. Biol.* 41:339.

59. Liu, Z.J., Xiao, M., Balint, K. *et al.* 2006. Notch1 signaling promotes primary melanoma progression by activating mitogen-activated protein kinase/phosphatidylinositol 3-kinase-Akt pathways and up-regulating N-cadherin

expression. *Cancer Res.* 66:4182.

60. Hurlbut, G.D., Kankel, M.W., Lake, R.J. and Artavanis-Tsakonas, S. 2007. Crossing paths with Notch in the hyper-network. *Curr. Opin. Cell Biol.* 19:166.

61. Konishi, J., Yi, F., Chen, X., Vo, H., Carbone, D.P. and Dang, T.P. 2009. Notch3 cooperates with the EGFR pathway to modulate apoptosis through the induction of bim. *Oncogene* 29:589.

62. Pallavi, S.K., Ho, D.M., Hicks, C., Miele, L. and Artavanis-Tsakonas, S. 2012. Notch and Mef2 synergize to promote proliferation and metastasis through JNK signal activation in Drosophila. *EMBO J.* 31:2895.

63. Xu, H., Zhu, J., Smith, S. *et al.* 2012. Notch-RBP-J signaling regulates the transcription factor IRF8 to promote inflammatory macrophage polarization. *Nat. Immunol.* 13:642.

64. Cheng, Y.L., Choi, Y., Seow, W.L. *et al.* 2014. Evidence that neuronal Notch-1 promotes JNK/c-Jun activation and cell death following ischemic stress. *Brain Res.* 1586:193.

65. Cook, B.D. and Evans, T. 2014. BMP signaling balances murine myeloid potential through SMAD-independent p38MAPK and NOTCH pathways. *Blood* 124:393.

66. Baeten, J.T. and Lilly, B. 2015. Differential regulation of NOTCH2 and NOTCH3 contribute to their unique functions in vascular smooth muscle cells. *J. Biol. Chem.* 290:16226.

67. Yee, N.S., Langen, H. and Besmer, P. 1993. Mechanism of kit ligand, phorbol ester, and calcium-induced down-regulation of c-kit receptors in mast cells. *J. Biol. Chem.* 268:14189.

68. Adachi, S., Tsujimura, T., Jippo, T. *et al.* 1995. Inhibition of attachment between cultured mast cells and fibroblasts by phorbol 12-myristate 13-acetate and stem cell factor. *Exp. Hematol.* 23:58.

69. Cruz, A.C., Frank, B.T., Edwards, S.T., Dazin, P.F., Peschon, J.J. and Fang, K.C. 2004. Tumor necrosis factor-alpha-converting enzyme controls surface expression of c-Kit and survival of embryonic stem cell-derived mast cells. *J. Biol. Chem.* 279:5612.

70. Broudy, V.C. 1997. Stem cell factor and hematopoiesis. *Blood* 90:1345.

71. Dahlen, D.D., Lin, N.L., Liu, Y.C. and Broudy, V.C. 2001. Soluble Kit receptor blocks stem cell factor bioactivity in vitro. *Leuk. Res.* 25:413.

72. Nijjar, S.S., Wallace, L., Crosby, H.A., Hubscher, S.G. and Strain, A.J. 2002. Altered Notch ligand expression in human liver disease: further evidence for a role of the Notch signaling pathway in hepatic neovascularization and biliary ductular defects. *Am. J. Pathol.* 160:1695.

73. Yabe, Y., Matsumoto, T., Tsurumoto, T. and Shindo, H. 2005. Immunohistological localization of Notch receptors and their ligands Delta and Jagged in synovial tissues of rheumatoid arthritis. *J. Orthop. Sci.* 10:589.

74. Niranjan, T., Bielesz, B., Gruenwald, A. *et al.* 2008. The Notch pathway in podocytes plays a role in the development of glomerular disease. *Nat. Med.* 14:290.

75. Fukuda, D., Aikawa, E., Swirski, F.K. *et al.* 2012. Notch ligand Delta-like 4 blockade attenuates atherosclerosis and metabolic disorders. *Proc. Natl. Acad. Sci. USA* 109:1868.

76. Syed, F. and Bayat, A. 2012. Notch signaling pathway in keloid disease: enhanced fibroblast activity in a Jagged-1 peptide-dependent manner in lesional vs. extralesional fibroblasts. *Wound Repair Regen.* 20:688.

77. Metz, M., Grimbaldeston, M.A., Nakae, S., Piliponsky, A.M., Tsai, M. and Galli, S.J. 2007. Mast cells in the promotion and limitation of chronic inflammation. *Immunol Rev.* 217:304.

78. Wang, W., Yu, S., Zimmerman, G. *et al.* 2015. Notch Receptor-Ligand Engagement Maintains Hematopoietic Stem Cell Quiescence and Niche Retention. *Stem Cells.*

33:2280.

79. Wang, W., Yu, S., Myers, J. *et al.* 2017. Notch2 blockade enhances hematopoietic stem cell mobilization and homing. *Haematologica.* 102:1785.

Figure legends

Figure 1. Adhesion of MCs to Notch ligand-transduced OP9 stromal cells was not inhibited by the insufficiency of Kit in MCs. (A) WT MCs were cultured on each OP9 stromal cell with 5 μg/ml of anti-IL-7Rα mAb (Ctrl mAb) or anti-Kit mAb (ACK2). The percentages of adherent MCs at each incubation time (5, 15, 30, 60, and 120 min) were shown. Data are the mean ± S.E. of triplicate cultures ($^{*}p < 0.05$ between Ctrl mAb and anti-Kit mAb at each time point, 2-tailed Welch's *t*-test). (B) Surface expression of Kit and FcεRIα on MCs-$Kit^{+/+}$ and -$Kit^{W\text{-}sh/W\text{-}sh}$. (C) Percentages of adherent MCs-$Kit^{+/+}$ and -$Kit^{W\text{-}sh/W\text{-}sh}$ on each OP9 stromal cell at 60 min of the adhesion assay were shown (mean ± S.E. of triplicate cultures. $^{*}p < 0.05$, 2-tailed Welch's *t*-test). (D) Surface expression of Notch1 and Notch2 on MCs-$Kit^{+/+}$ and -$Kit^{W\text{-}sh/W\text{-}sh}$, and Kit^{+} peritoneal MCs (See Supplemental Figure 2). (E) The expression of *Kit* and *Fcer1a* in the mixed lysates of adherent MCs-$Kit^{+/+}$ or -$Kit^{W\text{-}sh/W\text{-}sh}$ and each OP9 stromal cell after 60 min of the adhesion assay was analyzed by RT-PCR. RT-PCR with total RNAs from each MC alone before the adhesion assay was designated as 'Pre'. (F) The expression of *Kit*, *Fcer1a*, and *Kitl* in each OP9 stromal cell was analyzed by RT-PCR. (E, F) Original gel sources and negative controls are in Supplemental Figure 1.

Figure 2. Temporal changes in adhesion states of MCs on OP9 cells. (A) A representative photomicrograph of adherent MCs-$Kit^{+/+}$ on OP9-Dll4 cells after the removal of non-adherent MCs at 60 min of the adhesion assay. Scale bar; 50 μm. (B) (Left panels) Adhesion assay (60 min) for MCs-$Kit^{+/+}$ on OP9-Dll4 cells with the F-ATPase inhibitor NaN_3 (50 mM) or its solvent PBS (0.83% vol/vol) at 37°C or on ice. (Right panels) Adhesion assay (60 min) for MCs-$Kit^{+/+}$ on 2% PFA-fixed OP9-Dll4 cells with the actin polymerization inhibitor cytochalasin D (5 μM) or its solvent DMSO (0.05% vol/vol). Photomicrographs of adherent MCs were shown. Arrowhead: spreading MCs. (C, D) Adhesion assays for MCs-$Kit^{+/+}$ and MC-$Kit^{W\text{-}sh/W\text{-}sh}$ on OP9-Ctrl cells with various incubation times. (C) The ratios and (D) numbers of adherent MCs in each adhesion state in a well were shown. (E) Adhesion assays for MCs-$Kit^{+/+}$ with various incubation times on each OP9 transductant. Dotted lines indicate the total number of MCs plated in each well.

Figure 3. Spreading of adherent MCs on Notch ligand-transduced OP9 stromal cells was affected less by the insufficiency of Kit in MCs. (A and B) Adhesion assays (60 min) for MCs-$Kit^{+/+}$ and MCs-$Kit^{W\text{-}sh/W\text{-}sh}$ on each OP9 cell. (A) Representative

photomicrographs of adherent MCs. Scale bar; 50 μm. Arrowhead: spreading MCs. (B) The numbers of adherent MCs in each state were shown. (C) Adhesion assays (60 min) for MCs-*Kit*$^{+/+}$ on each OP9 cell with a control mAb (A7R34) or anti-Kit mAb (ACK2) (10 μg/ml each). (B and C) Data are the mean ± S.E. of triplicate cultures. Dotted lines indicate the total number of MCs plated on each well. Asterisks denote significant differences in each adhesion state between (B) MCs-*Kit*$^{+/+}$ and MCs-*Kit*$^{W\text{-}sh/W\text{-}sh}$ or (C) the control mAb and ACK2 ($p < 0.05$, 2-tailed Welch's *t*-test).

Figure 4. Spreading of adherent MCs-*Kit*$^{W\text{-}sh/W\text{-}sh}$ on Notch ligand-transduced OP9 stromal cells was dependent on the Notch receptor-ligand interaction, but independent of γ-secretase-mediated Notch signaling. (A) Adhesion assays (60 min) for MCs-*Kit*$^{W\text{-}sh/W\text{-}sh}$ on each OP9 cell with control pAb (20 μg/ml) or anti-Notch1 pAb plus anti-Notch2 pAb (10 μg/ml each). Cultures contained 76.9 μM NaN_3, which had no effect on the adhesion of MCs. (B) MCs-*Kit*$^{W\text{-}sh/W\text{-}sh}$ were pretreated with the γ-secretase inhibitor DAPT (50 μM) or its solvent DMSO (0.5% vol/vol) for 30 min, and the adhesion assay (60 min) was performed with the reagents. (C) MCs-*Kit*$^{+/+}$ were pretreated with an anti-Kit mAb (ACK2, 10 μg/ml) plus DAPT (30 μM) or DMSO (0.3% vol/vol) for 10 min, and the adhesion assay (60 min) was performed with the reagents. Data are the mean ± S.E. of triplicate cultures. Asterisks denote the significantly different responses of each adhesion state from control treatments ($p < 0.05$, 2-tailed Welch's *t*-test).

Figure 5. Kit- and Notch-dependent spreading of adherent MCs both involved MAPKs and PI3K signaling in MCs. (A-D) MCs-*Kit*$^{+/+}$ or MCs-*Kit*$^{W\text{-}sh/W\text{-}sh}$ were pretreated with SB203580 (p38 inhibitor, 50 μM), SP600125 (JNK inhibitor, 50 μM), PD98059 (MEK1/2 inhibitor, 50 μM), LY294002 (PI3K inhibitor, 20 μM), or the solvent DMSO (0.25% vol/vol) for 60 min, and adhesion assays (60 min) were performed with the reagents on the indicated OP9 stromal cells. Data are the mean ± S.E. of triplicate cultures. Asterisks denote the significantly different responses of each adhesion state from control treatments ($p < 0.05$, 1-tailed Welch's *t*-test). (D) Representative photomicrographs of adherent MC-*Kit*$^{W\text{-}sh/W\text{-}sh}$ under the indicated conditions in (B) and (C). Scale bar; 50 μm. Arrowhead; spreading MCs.

Figure 6. The Notch receptor-ligand interaction did not support the survival of MCs-*Kit*$^{W\text{-}sh/W\text{-}sh}$. MCs-*Kit*$^{+/+}$ and MCs-*Kit*$^{W\text{-}sh/W\text{-}sh}$ were cultured on each OP9 stromal cell for 7 days with the indicated reagents. Percent control responses of live MCs to day

0 (total MCs initially added) were shown. (A) The survival responses of each MC on each OP9 cell or without OP9 cells (OP9(-)). Data are the mean ± S.E. of triplicate cultures ($^{*}p < 0.05$, one-way ANOVA with Tukey's HSD test). Asterisks in the bars denote significant differences in the response on each OP9 cell from that on each OP9-Ctrl cell. (B) The responses of each MC on OP9-Ctrl cells with or without 10 μg/mL of an anti-CD4 mAb (GK1.5, for control) or anti-Kit mAb (ACK2). Data are the mean ± S.E. of triplicate cultures. $^{*}p < 0.05$, one-way ANOVA with Tukey's HSD test. n.s.: not significant. (C) The responses of MCs-*Kit*$^{+/+}$ on OP9-Ctrl cells with SB203580 (SB, 40 μM), PD98059 (PD, 40 μM), LY294002 (LY, 20 μM), or the solvent DMSO (0.2% vol/vol). Data are the mean ± S.E. of triplicate cultures. $^{*}p < 0.05$, one-way ANOVA with 2-tailed Dunnett's pairwise multiple comparison *t*-test.

Figure 7. Summary of Kit- and Notch-mediated cell adhesion. The tethering of MCs to stromal cells is induced by Kit-Kitl and Notch receptor-ligand interactions (26). Kit signaling activates the PI3K and MAPKs pathways, leading to the induction of integrin activation and cytoskeletal reorganization, which enables MCs to spread (15-24). The Notch-mediated tethering of MCs leads to the activation of the above signaling pathway that induces the spreading of adherent MCs as Kit-mediated adhesion, in a manner independent of the γ-secretase activity. The mechanisms by which the PI3K and MAPKs pathways are activated during Notch-mediated adhesion remain unclear; however, γ-secretase-independent non-canonical Notch signaling (50-52) may be involved: (A), non-canonical signaling may directly activate PI3K (53-55), and (B) Notch signaling may indirectly influence signaling from other RTKs to modulate the activation of MAPKs (56-66). Kit supports the adhesion and survival of MCs, whereas Notch only supports adhesion (Table).

Figure 1

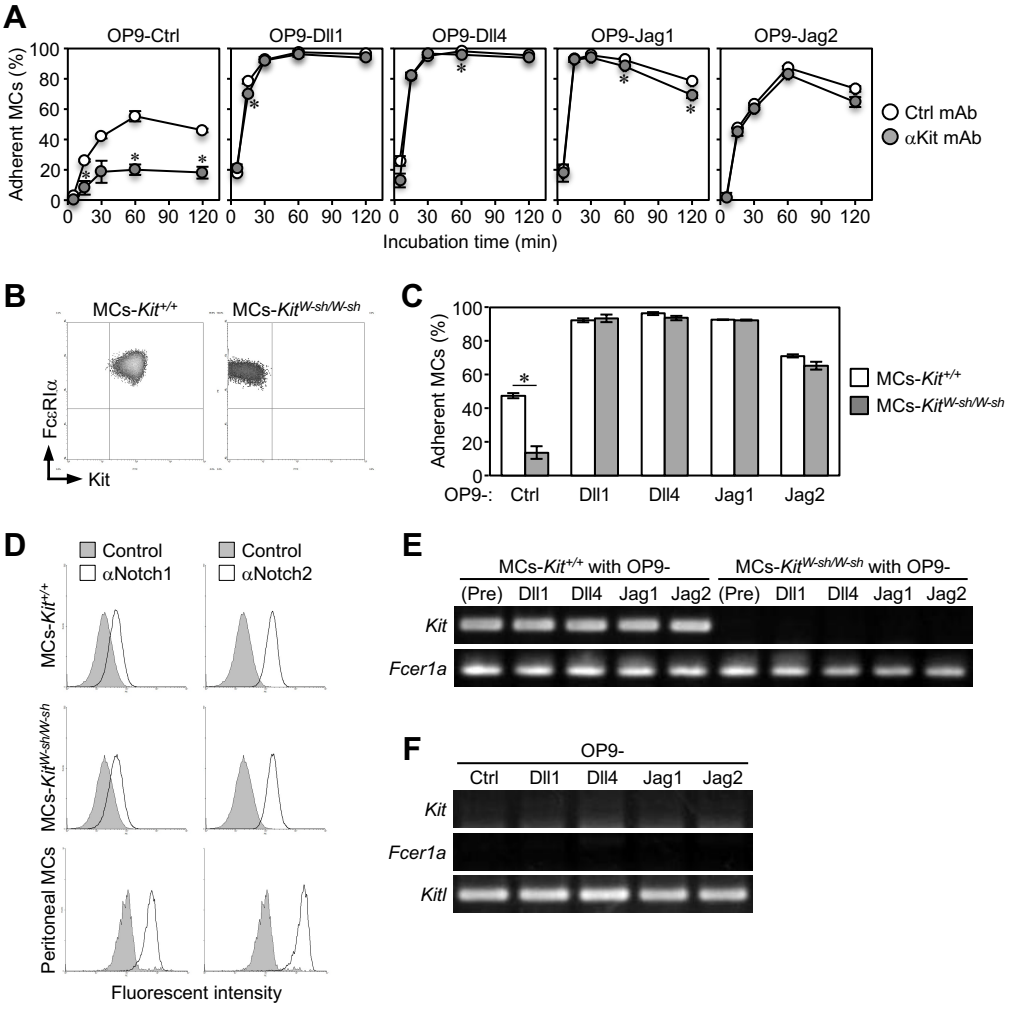
A
OP9-Ctrl
OP9-Dll1
OP9-Dll4
OP9-Jag1
OP9-Jag2
Adherent MCs (%)
Incubation time (min)
Ctrl mAb
αKit mAb
B
MCs-Kit+/+
MCs-KitW-sh/W-sh
FcεRIα
Kit
C
Adherent MCs (%)
OP9-: Ctrl Dll1 Dll4 Jag1 Jag2
MCs-Kit+/+
MCs-KitW-sh/W-sh
D
Control
αNotch1
Control
αNotch2
MCs-Kit+/+
MCs-KitW-sh/W-sh
Peritoneal MCs
Fluorescent intensity
E
MCs-Kit+/+ with OP9-
MCs-KitW-sh/W-sh with OP9-
(Pre) Dll1 Dll4 Jag1 Jag2 (Pre) Dll1 Dll4 Jag1 Jag2
Kit
Fcer1a
F
OP9-
Ctrl Dll1 Dll4 Jag1 Jag2
Kit
Fcer1a
Kitl

Figure 2

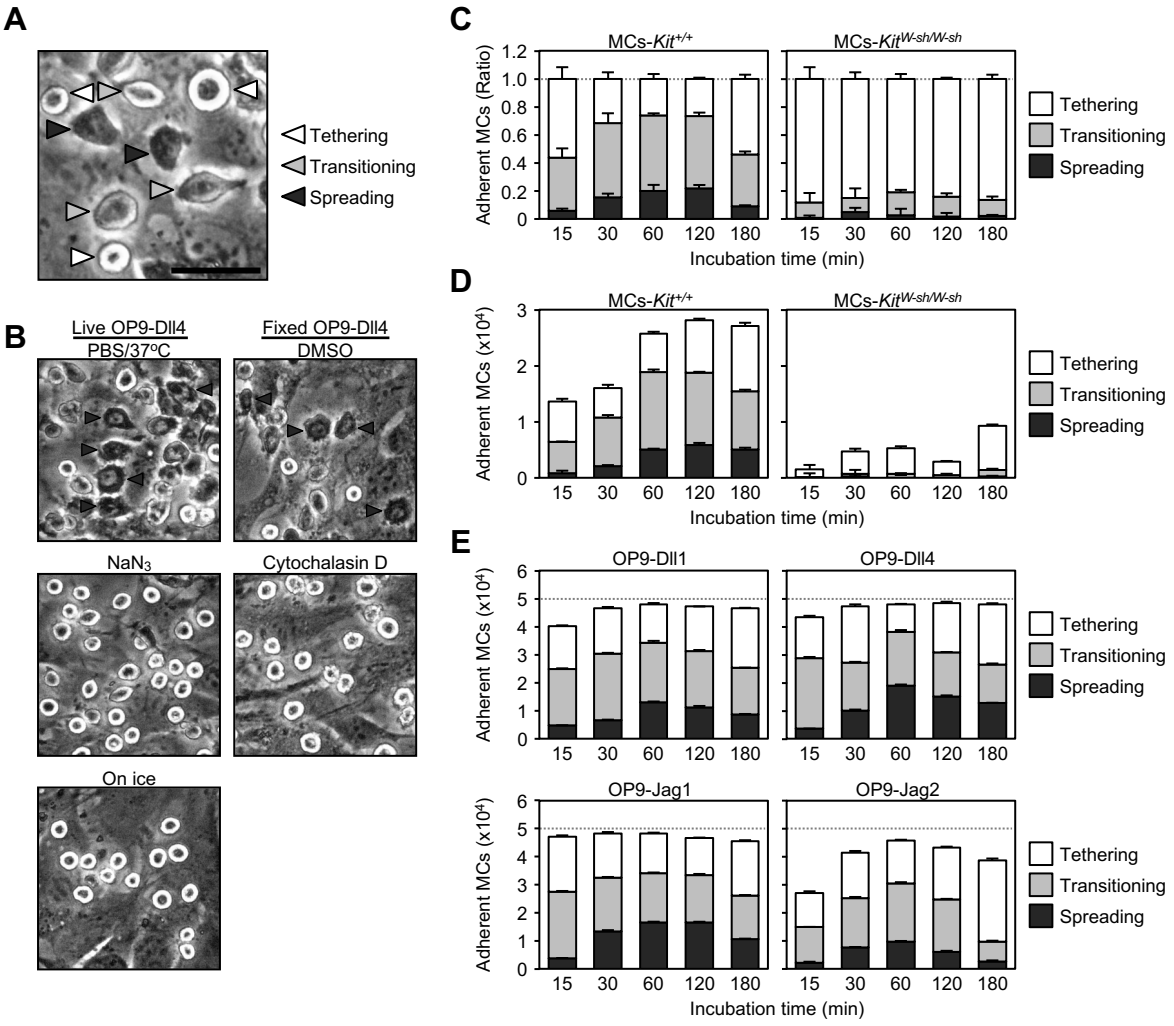
A
Tethering
Transitioning
Spreading
B
Live OP9-Dll4
PBS/37ºC
Fixed OP9-Dll4
DMSO
NaN3
Cytochalasin D
On ice
C
MCs-Kit+/+
MCs-KitW-sh/W-sh
Adherent MCs (Ratio)
Incubation time (min)
Tethering
Transitioning
Spreading
D
MCs-Kit+/+
MCs-KitW-sh/W-sh
Adherent MCs (x10⁴)
Incubation time (min)
Tethering
Transitioning
Spreading
E
OP9-Dll1
OP9-Dll4
OP9-Jag1
OP9-Jag2
Adherent MCs (x10⁴)
Incubation time (min)
Tethering
Transitioning
Spreading

Figure 3

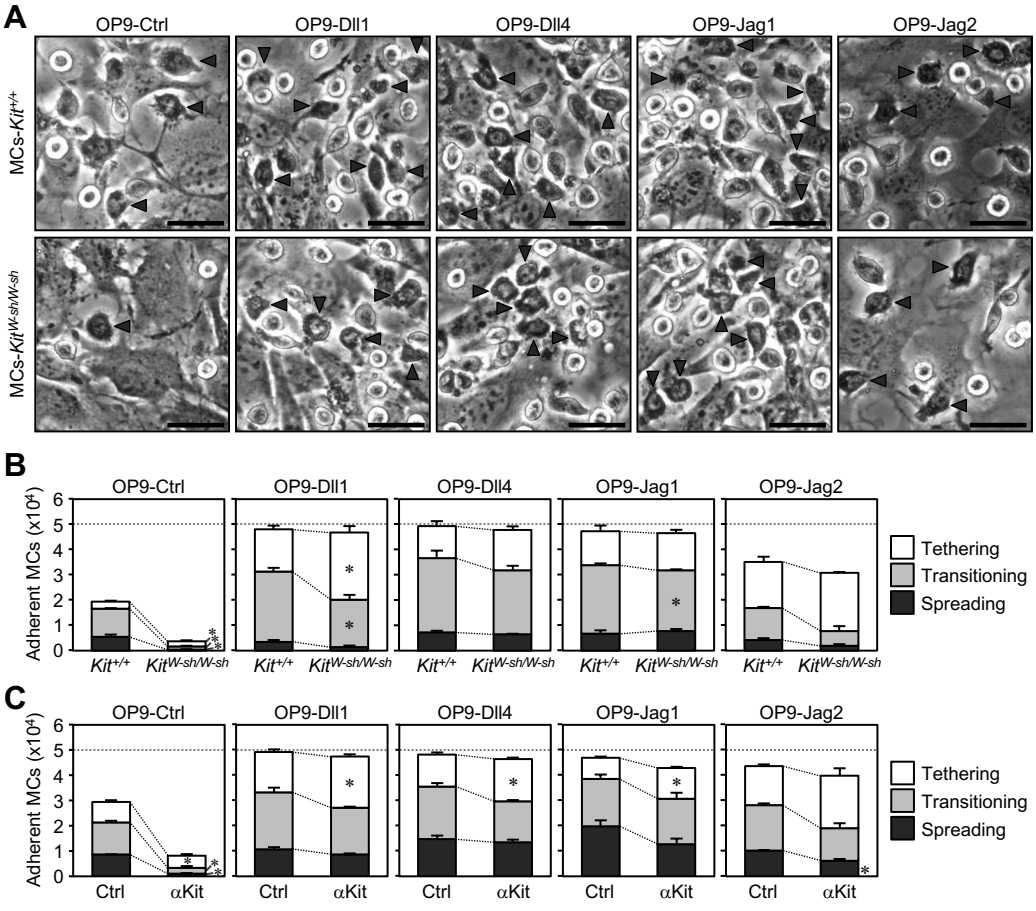
A
OP9-Ctrl
OP9-Dll1
OP9-Dll4
OP9-Jag1
OP9-Jag2
MCs-Kit+/+
MCs-KitW-sh/W-sh
B
OP9-Ctrl
OP9-Dll1
OP9-Dll4
OP9-Jag1
OP9-Jag2
Adherent MCs (x10⁴)
Kit+/+
KitW-sh/W-sh
Tethering
Transitioning
Spreading
C
OP9-Ctrl
OP9-Dll1
OP9-Dll4
OP9-Jag1
OP9-Jag2
Adherent MCs (x10⁴)
Ctrl
αKit
Tethering
Transitioning
Spreading

Figure 4

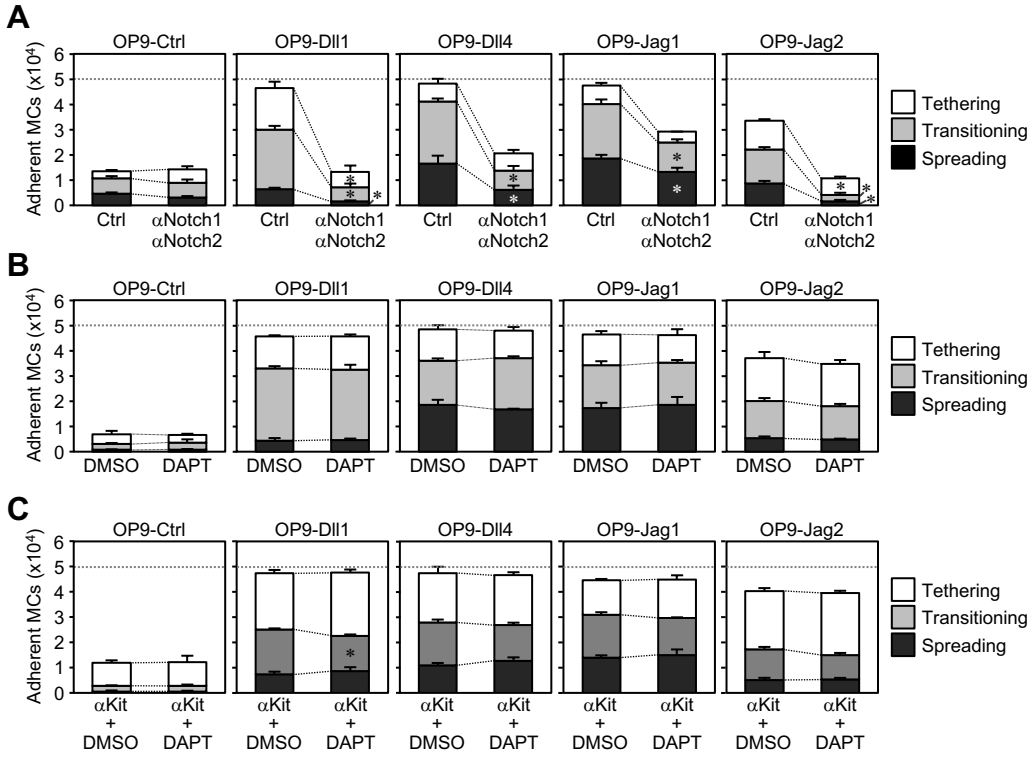
A
OP9-Ctrl
OP9-Dll1
OP9-Dll4
OP9-Jag1
OP9-Jag2
Adherent MCs (x10⁴)
0
1
2
3
4
5
6
Ctrl
αNotch1
αNotch2
Tethering
Transitioning
Spreading
B
DMSO
DAPT
C
αKit
+
DMSO
αKit
+
DAPT

Figure 5

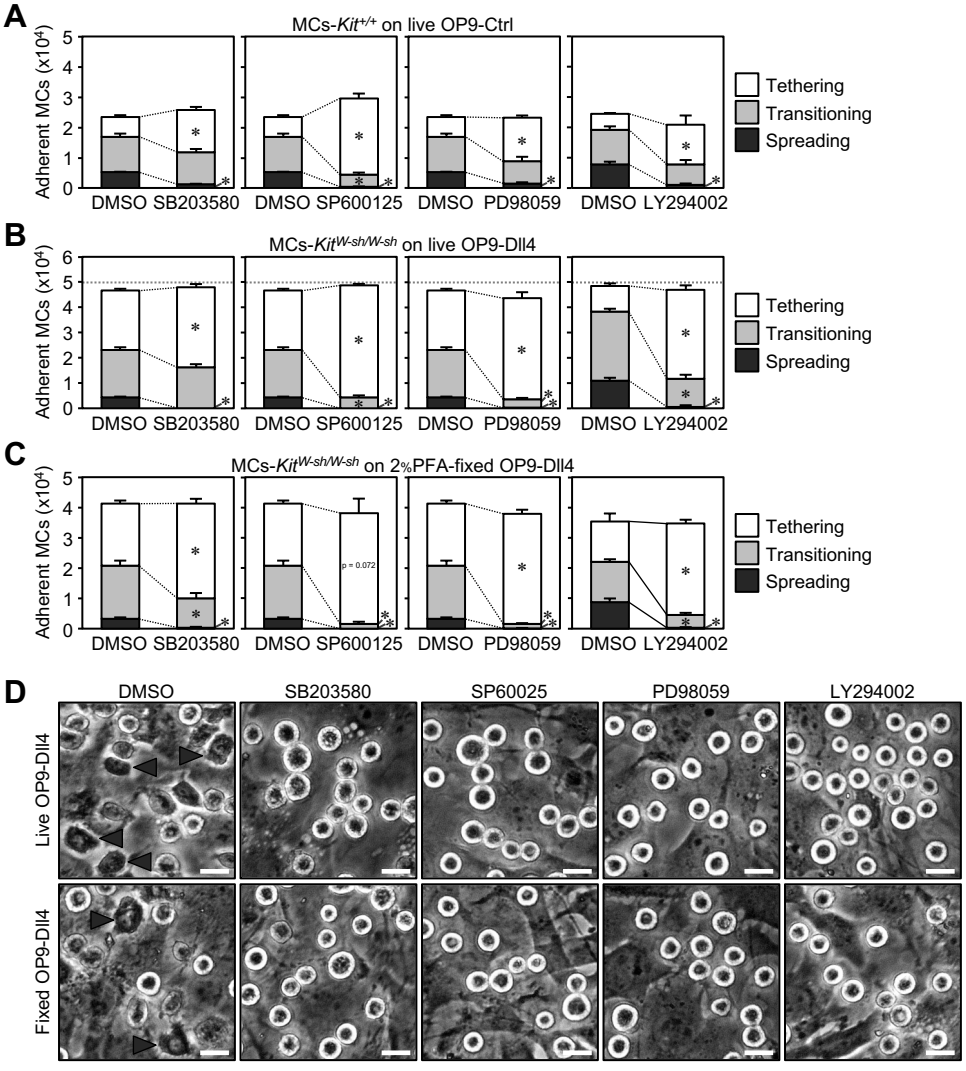
A
MCs-Kit+/+ on live OP9-Ctrl
Adherent MCs (x10⁴)
Tethering
Transitioning
Spreading
DMSO SB203580 DMSO SP600125 DMSO PD98059 DMSO LY294002
B
MCs-KitW-sh/W-sh on live OP9-Dll4
C
MCs-KitW-sh/W-sh on 2%PFA-fixed OP9-Dll4
p = 0.072
D
DMSO
SB203580
SP60025
PD98059
LY294002
Live OP9-Dll4
Fixed OP9-Dll4

Figure 6

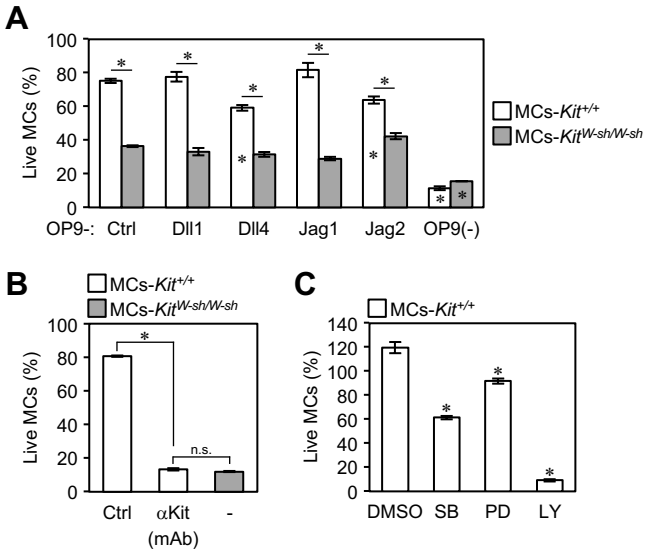
A
Live MCs (%)
100
80
60
40
20
0
OP9-: Ctrl Dll1 Dll4 Jag1 Jag2 OP9(-)
MCs-Kit+/+
MCs-KitW-sh/W-sh
B
MCs-Kit+/+
MCs-KitW-sh/W-sh
Live MCs (%)
n.s.
Ctrl αKit (mAb) -
C
MCs-Kit+/+
Live MCs (%)
140
120
100
80
60
40
20
0
DMSO SB PD LY

Figure 7

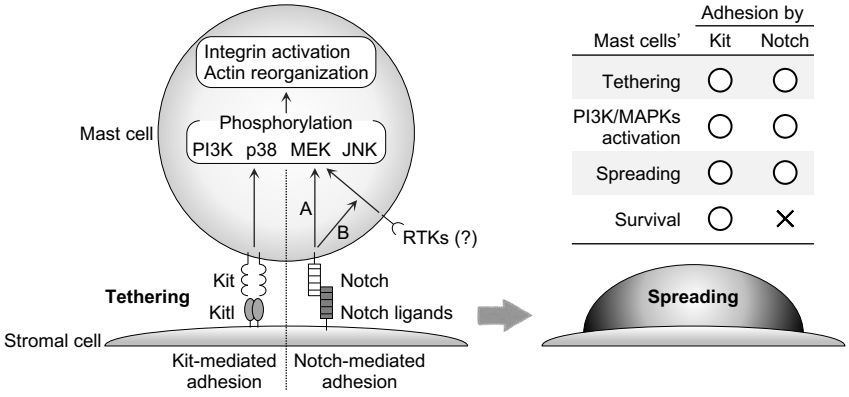

Mast cells'	Adhesion by Kit	Adhesion by Notch
Tethering	○	○
PI3K/MAPKs activation	○	○
Spreading	○	○
Survival	○	×

Supplemental Figure 1

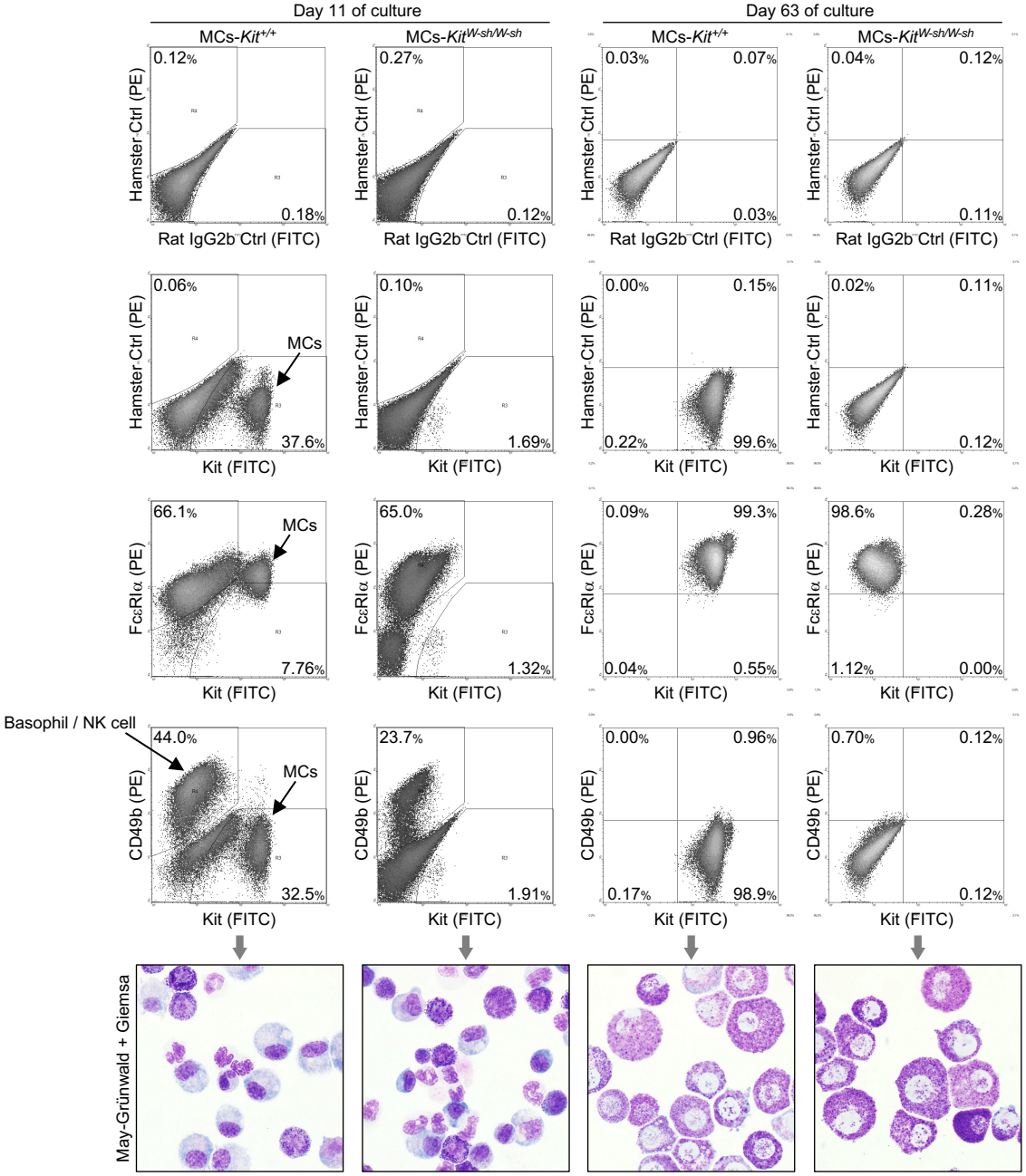

Fig. S1. MCs-*Kit*$^{W\text{-}sh/W\text{-}sh}$ are MCs, not basophils.

On days 11 and 63 of the induction of MCs from the bone marrow cells of C57BL/6-*Kit*$^{+/+}$ and -*Kit*$^{W\text{-}sh/W\text{-}sh}$ mice, the expression of Kit, FcεRIα, and CD49b (DX5, basophil, and NK cell marker) was analyzed by flow cytometry. On day 11 of the MCs-*Kit*$^{+/+}$ culture, when MCs and basophils co-exist (I), CD49b^{+} cells were detected in the Kit^{-} fraction, whereas Kit^{+} cells were FcεRIα^{+}CD49b^{-}. The MCs-*Kit*$^{W\text{-}sh/W\text{-}sh}$ culture also contained CD49b^{+} cells. On day 63 of both cultures, most of the cells were FcεRIα^{+}CD49b^{-}. Histocytochemistry with May-Grünwald and Giemsa solution (Muto Pure Chemicals, Tokyo, Japan) showed that all cells in both cultures on day 63 had similar morphologies and granulation, suggesting that cells in both cultures are MCs.

I. Ohnmacht, C., and Voehringer, D. 2009.
Basophil effector function and homeostasis during helminth infection. *Blood* 113:2816.

Supplemental Figure 2

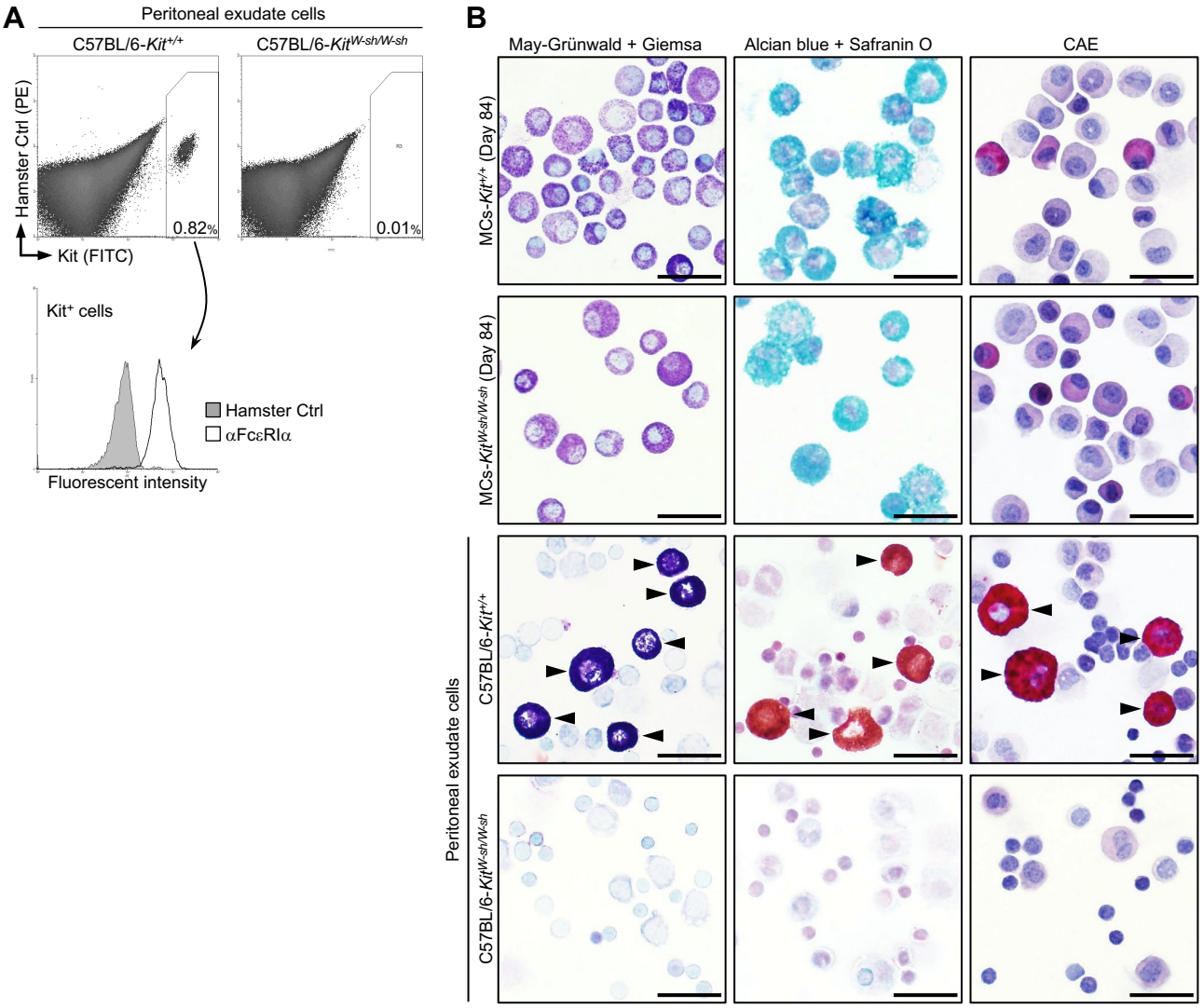

Fig. S2. Staining of Peritoneal MCs and bone marrow-derived MCs

(A) Detection of peritoneal mast cells (related to Figure 1D). Kit^{hi} cells in the peritoneal exudate cells of C57BL/6-*Kit*$^{+/+}$ mice expressed FcεRIα. MC-deficient C57BL/6-*Kit*$^{W\text{-}sh/W\text{-}sh}$ mice lacked this population, suggesting that they are MCs. (B) Histocytochemistry of MCs-*Kit*$^{+/+}$ and -*Kit*$^{W\text{-}sh/W\text{-}sh}$ (84 days of culture) and peritoneal exudate cells from C57BL/6-*Kit*$^{+/+}$ and -*Kit*$^{W\text{-}sh/W\text{-}sh}$ mice. Alcian blue + Safranin O: cells were initially stained with Alcian blue (pH 2.5), and then with 0.1% safranin O (Muto Pure Chemicals). Naphthol AS-D chloroacetate esterase (CAE): Cells were stained with CAE staining kit (Sigma-Aldrich) according to the manufacturer's instruction. Peritoneal MCs (C57BL/6-*Kit*$^{+/+}$) were mature connective tissue-type MCs (II), as shown by red staining with safranin O and CAE staining (red) (III). In contrast, MCs-*Kit*$^{+/+}$ and -*Kit*$^{W\text{-}sh/W\text{-}sh}$ were immature mucosal-type MCs (II), as shown by blue staining with Alcian blue and weak to negative staining with CAE. Arrows: peritoneal MCs. Bars: 25 μm.

II. Gurish, M.F. and Austen, K.F. 2012.
Developmental origin and functional specialization of mast cell subsets. *Immunity* 37:25.

III. Fukao, T., Yamada, T., Tanabe, M. *et al.* 2002.
Selective loss of gastrointestinal mast cells and impaired immunity in PI3K-deficient mice. *Nat. Immunol.* 3:295.

Supplemental Figure 3

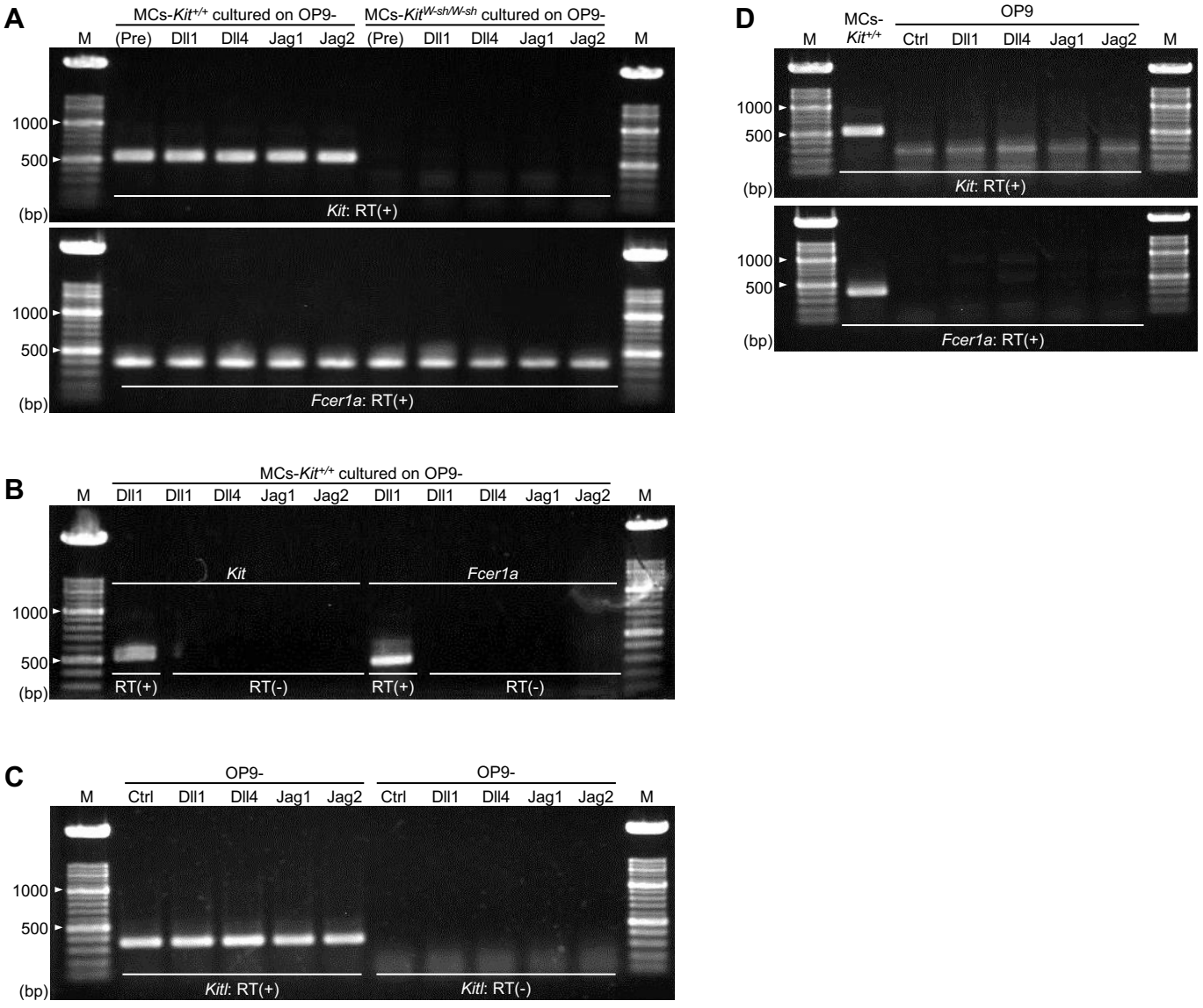

Fig. S3. Original gel sources and negative controls related to Figures 1E and 1F.

(A) Original gel sources for Figure 1E. (B) Negative control for the RT-PCR analysis related to Figure 1E and (A). RT(-) denotes PCR with total RNA subjected to the reverse-transcription reaction without a RT enzyme. (C) Original gel source and the negative control for *Kitl* in Figure 1F. (D) Original gel source for *Kit* and *Fcer1a* in Figure 1F.

Supplemental Figure 4

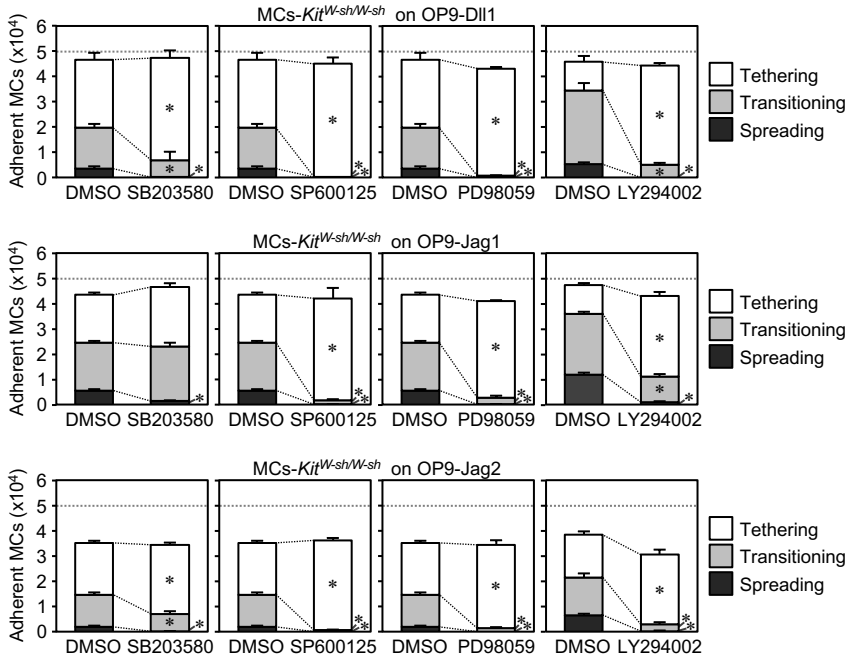

Fig. S4. Notch-dependent spreading of adherent MCs-*Kit*$^{W\text{-}sh/W\text{-}sh}$ involved MAPKs and PI3K signaling in MCs.

MCs-*Kit*$^{W\text{-}sh/W\text{-}sh}$ were pretreated with SB203580 (p38 inhibitor, 50 μM), SP600125 (JNK inhibitor, 50 μM), PD98059 (MEK1/2 inhibitor, 50 μM), LY294002 (PI3K inhibitor, 20 μM), or the solvent DMSO (0.25% vol/vol) for 60 min, and adhesion assays (60 min) were performed with the reagents on the indicated OP9 stromal cells. Dotted lines indicate the total number of MCs plated on the wells. Asterisks denote the significantly different responses of each adhesion state from control treatments ($p < 0.05$, 1-tailed Welch's *t*-test).

Supplemental Figure 5

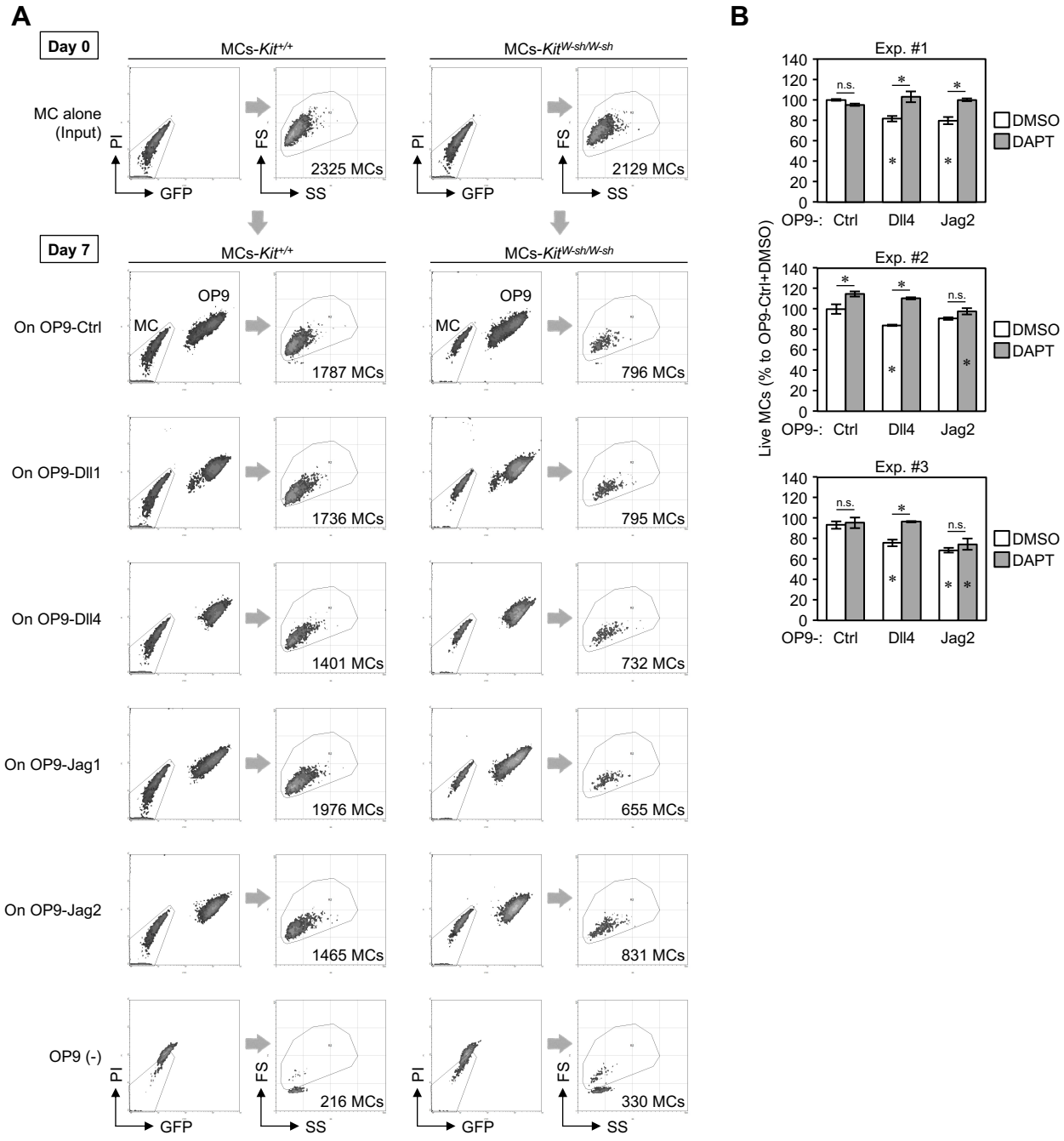

Fig. S5. Notch signaling may negatively affect the survival of MCs-*Kit*$^{+/+}$ on OP9-Dll4 and -Jag2.

(A) Detection of live MCs after a 7-day co-culture with each OP9 stromal cell by flow cytometry. On day 7 of the co-culture, all cells in the wells were harvested with trypsinization, stained with PI, and analyzed by flow cytometry. GFP$^-$PI$^-$ cells in the 60-second flow were counted as live MCs. Representative histograms were shown. (B) MCs-*Kit*$^{+/+}$ were cultured on the indicated OP9 cell for 7 days with DAPT (20 μM) or the same volume of DMSO (0.1% vol/vol), and the number of surviving MCs was analyzed. Percent control responses to the response of OP9-Ctrl+DMSO in 3 independent experiments were shown. Data are the mean ± S.E. of triplicate cultures. $^*p < 0.05$, one-way ANOVA with Tukey's HSD test. n.s.: not significant. Asterisks in the bars indicate significant differences from each response on OP9-Ctrl.

Supplemental Figure 6

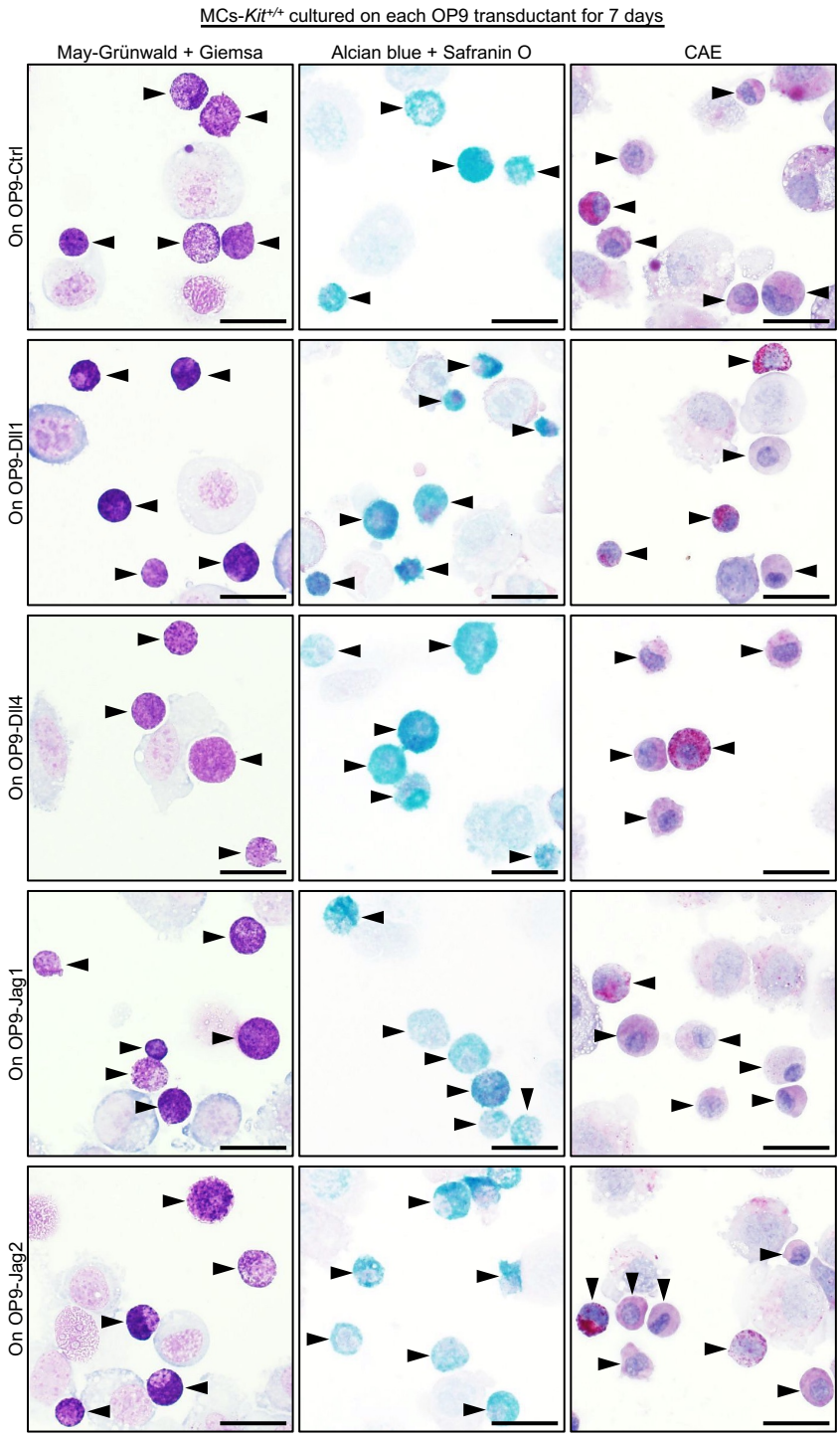

Fig. S6. Granule contents of MCs-*Kit*$^{+/+}$ did not show marked changes after a co-culture with each OP9 transductant.

After culturing MCs-*Kit*$^{+/+}$ on each OP9 transductant for 7 days, cells (OP9 cells + MCs) were harvested and stained with the indicated reagents. Co-cultured MCs-*Kit*$^{+/+}$ still showed blue staining with Alcian blue and weak to negative staining with CAE, suggesting that Notch-mediated cell adhesion did not influence the maturation of MCs-*Kit*$^{+/+}$ during the co-culture (compare with peritoneal mature MCs in Supplemental Figure 2). Arrows: MCs. Bars: 25 μm.